#### **MATERIALS SCIENCE**

# Dropwise condensation on solid hydrophilic surfaces

Hyeongyun Cha<sup>1,2</sup>\*, Hamed Vahabi<sup>3</sup>\*, Alex Wu<sup>1</sup>, Shreyas Chavan<sup>1</sup>, Moon-Kyung Kim<sup>1</sup>, Soumyadip Sett<sup>1</sup>, Stephen A. Bosch<sup>1</sup>, Wei Wang<sup>3</sup>, Arun K. Kota<sup>3,4,5,6†</sup>, Nenad Miljkovic<sup>1,2,7,8†</sup>

Droplet nucleation and condensation are ubiquitous phenomena in nature and industry. Over the past century, research has shown dropwise condensation heat transfer on nonwetting surfaces to be an order of magnitude higher than filmwise condensation heat transfer on wetting substrates. However, the necessity for nonwetting to achieve dropwise condensation is unclear. This article reports stable dropwise condensation on a smooth, solid, hydrophilic surface ( $\theta_a = 38^\circ$ ) having low contact angle hysteresis (<3°). We show that the distribution of nano- to micro- to macroscale droplet sizes (about 100 nm to 1 mm) for coalescing droplets agrees well with the classical distribution on hydrophobic surfaces and elucidate that the wettability-governed dropwise-to-filmwise transition is mediated by the departing droplet Bond number. Our findings demonstrate that achieving stable dropwise condensation is not governed by surface intrinsic wettability, as assumed for the past eight decades, but rather, it is dictated by contact angle hysteresis.

Copyright © 2020
The Authors, some rights reserved; exclusive licensee American Association for the Advancement of Science. No claim to original U.S. Government Works. Distributed under a Creative Commons Attribution NonCommercial License 4.0 (CC BY-NC).

#### INTRODUCTION

Droplet nucleation and condensation are ubiquitous phenomena in nature and industry. Over the past century, research has shown that heat transfer rates during steam dropwise condensation on nonwetting (e.g., hydrophobic) surfaces can be 10× higher than widely accepted filmwise condensation on wetting substrates (1-4). However, the need for nonwetting hydrophobic coatings in achieving dropwise condensation of water is unclear. Sustained dropwise condensation requires high droplet mobility to achieve continuous droplet removal from the surface. The mobility of a droplet on homogeneous and heterogeneous surfaces is governed mainly by the contact angle hysteresis (i.e., the difference between the advancing and receding contact angles) (5-10) rather than the intrinsic wettability. While all prior work on achieving dropwise condensation has focused on using hydrophobic surfaces, we postulate that achieving stable dropwise condensation on a solid hydrophilic surface with low contact angle hysteresis is theoretically possible.

Dropwise condensation on hydrophilic surfaces has additional advantages including enhanced nucleation (Fig. 1A) due to reduced energy barriers for heterogeneous nucleation (Fig. 1B) (11), lower conduction thermal resistance (12), and higher (~500%) heat transfer coefficient (Fig. 1C). Furthermore, droplet shedding and mobility due to gravitational forces become invariant to intrinsic surface wettability as the contact angle hysteresis approaches zero (Fig. 1D), ensuring that high heat transfer is maintained even for solid hydrophilic substrates (Fig. 1E).

In this study, we report the first observation of stable dropwise condensation on a solid PEGylated surface having subnanoscale

roughness and extreme chemical homogeneity, resulting in hydrophilic behavior ( $\theta_a = 38^\circ$ ) with minimal contact angle hysteresis (<3°). We studied the nucleation site distribution on the hydrophilic substrate during water vapor condensation, showing that the distribution of droplet sizes from nano- to micro- to macroscale (about 100 nm to 1 mm) for coalescing droplets agrees remarkably well with the classical Rose distribution on hydrophobic surfaces. On the basis of our experimental findings, we developed a physical model to show that stable dropwise condensation, rather than being governed by the surface intrinsic wettability or advancing contact angle, as assumed for the past eight decades (1), is mainly dictated by the contact angle hysteresis. This work not only provides fundamental insights into dropwise condensation theory but also demonstrates a previously unexplored avenue of using durable and wetting inorganic surfaces with subnanoscale roughness and extreme chemical homogeneity to achieve high droplet mobility.

#### **RESULTS**

#### **Hydrophilic surface**

Maintaining a high intrinsic wettability (i.e.,  $\theta_a \ll 90^\circ$ ) with minimal contact angle hysteresis is difficult to achieve. Many studies have noted the formation of discrete "flat" water droplets on hydrophilic substrates during condensation due to atmospheric contamination of volatile organic compounds (VOCs) after cleaning (13, 14); however, the corresponding receding contact angle is typically close to zero (15), resulting in filmwise condensation (16). Hence, for the past eight decades, dropwise condensation of water has been achieved mainly via the deposition of hydrophobic conformal coatings. However, as the contact angle hysteresis approaches zero, the minimum droplet sliding size becomes invariant to intrinsic surface wettability (Fig. 1D). We postulate that the performance of hydrophilic surfaces with low contact angle hysteresis in dropwise condensation is at least comparable to that of hydrophobic surfaces.

To experimentally reconcile our predictions and to investigate the mechanism governing stable dropwise condensation, we fabricated solid, smooth, slippery hydrophilic surfaces through PEGylation of silicon wafers (see Materials and Methods and section S1). Our PEGylated surfaces enable the formation of water droplets with relatively low intrinsic advancing contact angles, while maintaining minimal

<sup>&</sup>lt;sup>1</sup>Department of Mechanical Science and Engineering, University of Illinois at Urbana-Champaign, Urbana, IL 61801, USA. <sup>2</sup>International Institute for Carbon Neutral Energy Research (WPI-12CNER), Kyushu University, 744 Moto-oka, Nishi-ku, Fukuoka 819-0395, Japan. <sup>3</sup>Department of Mechanical Engineering, Colorado State University, Fort Collins, CO 80523, USA. <sup>4</sup>School of Biomedical Engineering, Colorado State University, Fort Collins, CO 80523, USA. <sup>5</sup>Department of Chemical Engineering, Colorado State University, Fort Collins, CO 80523, USA. <sup>6</sup>Department of Mechanical and Aerospace Engineering, North Carolina State University, Raleigh, NC 27695, USA. <sup>7</sup>Materials Research Laboratory, University of Illinois at Urbana-Champaign, Urbana, IL 61801, USA. <sup>8</sup>Department of Electrical and Computer Engineering, University of Illinois at Urbana-Champaign, Urbana, IL 61801, USA.

<sup>\*</sup>These authors contributed equally to this work.

<sup>†</sup>Corresponding author. Email: akota2@ncsu.edu (A.K.K.); nmiljkov@illinois.edu (N.M.)

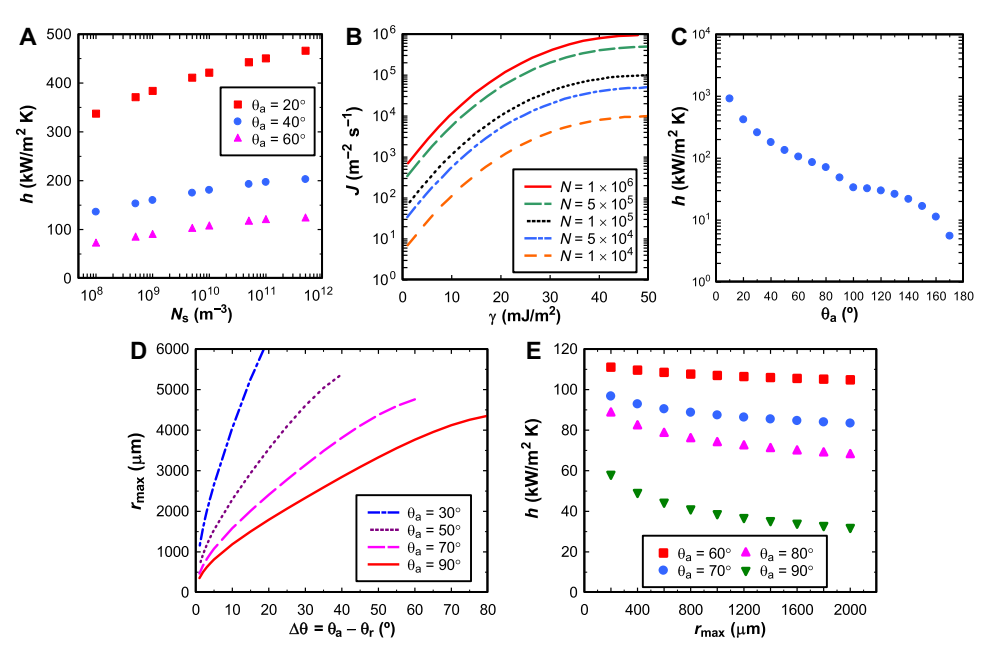


**Fig. 1. Parameters affecting condensation heat transfer coefficient (h).** (**A**) Model results of h as a function of nucleation density ( $N_s$ ) for varying advancing contact angle ( $\theta_a$ ) with departure radius  $r_{max} = 1$  mm. (**B**) Condensation nucleation rate (J) as a function of condensing surface energy (γ). (**C**) h as a function of  $\theta_a$  with  $N_s = 5 \times 10^{10}$  m<sup>-2</sup> and  $r_{max} = 1$  mm. (**D**) Theoretical  $r_{max}$  as a function of contact angle hysteresis (Δθ). (**E**) h as a function of  $r_{max}$  for varying  $\theta_a$  with  $N_s = 5 \times 10^{10}$  m<sup>-2</sup>. The results assume a vapor pressure of 3500 Pa and a surface temperature of 20°C. Results show that hydrophilic dropwise condensation is advantageous to hydrophobic.

contact angle hysteresis ( $\Delta\theta = \theta_a - \theta_r$ ). Macroscopic water droplets deposited on our precisely engineered PEGylated surfaces displayed advancing and receding contact angles of  $\theta_a = 38^{\circ} \pm 1^{\circ}$  and  $\theta_r =$  $35^{\circ} \pm 1^{\circ}$ , respectively ( $\Delta\theta \approx 3^{\circ}$ ; Fig. 2A) (5). Microscale goniometric measurements of droplets on our PEGylated silicon wafer showed  $\theta_a$  = 38.6°  $\pm$  0.6° and  $\theta_r$  = 36°  $\pm$  0.7°, respectively ( $\Delta\theta\approx 2^\circ$ ). The low contact angle hysteresis on our PEGvlated surfaces is due to the high degree of chemical homogeneity (i.e., uniform surface modification) and physical homogeneity (i.e., low surface roughness) (6, 7, 17). High-resolution C 1s x-ray photoelectron spectroscopy (XPS) spectra (Fig. 2B) at >30 locations showed the presence of a peak at 286.5 eV corresponding to the -C-O bond, implying excellent chemical homogeneity (18). Further, atomic force microscopy (AFM) showed a low root mean square roughness,  $R_{\rm rms} \approx 0.25$  nm (Fig. 2C), implying a high degree of physical homogeneity. Ellipsometry revealed that our PEGylated coatings were <1 nm thick.

Although the recent development of lubricant-infused surfaces (LISs) or slippery liquid-infused porous surfaces (SLIPSs) has shown the concurrent minimization of intrinsic contact angle and hysteresis for low–surface tension condensates (19, 20), this was not achieved with water, which still showed hydrophobic states ( $\theta_a > 90^\circ$ ) (12, 21). Furthermore, although past studies have shown the presence of apparent hydrophilic-state droplets ( $\theta_a \approx 60^\circ$ ) during water vapor condensation on LISs (22), the apparent droplet-surface contact beneath the lubricant was hydrophobic ( $\theta_a > 90^\circ$ ) (23, 24), resulting in enhanced droplet shedding mainly due to lowering of the droplet-air interfacial tension via the conversion to a droplet-lubricant interface. Last, LISs and SLIPSs can suffer from miscibility, cloaking, and drainage degradation mechanisms not present on solid surfaces (25).

#### Hydrophilic versus hydrophobic

The nucleation, growth, and coalescence of condensing water droplets were studied by condensing water vapor either from the ambient laboratory environment or from a saturated vapor supply on our surfaces having temperatures  $T_{\rm w}=5^{\circ}\pm0.5^{\circ}{\rm C}$ . Details of the experimental setup can be found elsewhere (26). To compare the condensation dynamics on our PEGylated hydrophilic surfaces with classical dropwise condensation dynamics on hydrophobic surfaces, we also fabricated similar smooth silicon surfaces functionalized with a fluorinated polymer (C<sub>4</sub>F<sub>8</sub>) deposited using chemical vapor deposition under low pressure at room temperature. Microscale goniometric measurements of water droplets on the smooth hydrophobic silicon wafer showed  $\theta_a=110^{\circ}\pm4^{\circ}$  and  $\theta_r=102^{\circ}\pm5^{\circ}$ , respectively.

Droplet nucleation studies using optical microscopy revealed the formation of discrete droplets on our hydrophilic PEGylated surfaces. Details of the optical microscopy setup can be found elsewhere (14, 27, 28). Because of the hydrophilic nature of the surface, the initial nucleation density, before droplet coalescence mediated growth, was one order of magnitude higher on the hydrophilic surface ( $n \le$  $2.23 \times 10^{10}$  droplets/m<sup>2</sup>) when compared to the hydrophobic reference  $(n \le 2.47 \times 10^9 \text{ droplets/m}^2)$ , in agreement with classical nucleation theory (11) and as observed in previous experimental studies of heterogeneous condensation of ambient water vapor on biphilic surfaces (29, 30). Once droplet coalescence initiated between neighboring droplets on our hydrophilic PEGylated surface, analogous transitions to larger discrete droplets ensued, and dropwise condensation was maintained (fig. S1). Upon coalescence, the three-phase contact line was able to depin because of the ultralow contact angle hysteresis and maintain circular contact lines. To study the behavior of interacting hydrophilic droplets, we elevated the nucleation density on our PEGylated surface by increasing the saturation temperature of the incoming saturated ( $\Phi = 100\%$ ) vapor supply to  $T_{air} = 35^{\circ} \pm 0.5^{\circ}$ C. The higher saturation temperature increased the supersaturation  $(S = [\Phi P_{\text{sat}}(T_{\text{air}})]/P_{\text{sat}}(T_{\text{w}}))$  from  $S = 1.02 \pm 0.035$  to  $S = 6.45 \pm 0.4$ , with a corresponding increase in the nucleation density to  $N \ge 4 \times 10^{12}$ , consistent with nucleation site activation (11). At the elevated densities,

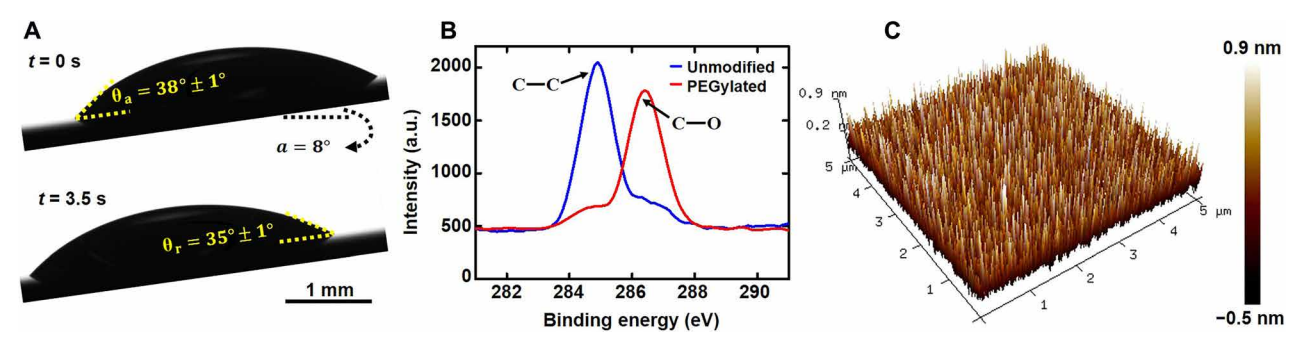


**Fig. 2. Surface characteristics and wettability.** (**A**) Images showing a water droplet sliding across our PEGylated surfaces tilted by 8° relative to the horizontal. (**B**) High-resolution C 1s XPS spectra of the unmodified and our PEGylated surfaces. The —C—C peak on an unmodified silicon wafer is due to adventitious carbon. The —C—O peak on our PEGylated surface is indicative of PEGylation. a.u., arbitrary units. (**C**) AFM image depicting the topography of our PEGylated surface with root mean square roughness,  $R_{rms} < 1$  nm, and thickness < 1 nm.

the center-to-center spacing between neighboring droplets was as low as  $\approx$ 500 nm. Unexpectedly, the formation of discrete nanoscale droplets was stable on our hydrophilic PEGylated surface, with droplets having radii as small as  $R = 300 \pm 150$  nm.

To study the scale dependency of discrete droplet formation and stability of dropwise condensation, we quantified the droplet distribution for nano- to macroscale droplets during condensation on a vertical flat plate. The experimental setup is described elsewhere (26). Briefly, the sample is cooled to  $0.05^{\circ} \pm 0.1^{\circ}$ C. Saturated water vapor was sparged from a second water bath of deionized (DI) water at  $73^{\circ} \pm 3^{\circ}$ C. The resulting condensation area spanned roughly 2.5 cm horizontally and 1 cm vertically and represented the topmost area of a vertical pate. To capture droplet data during all stages of a sweeping period and to ensure statistical significance, we captured one image every 20 s. Figure 3 shows the self-similar nature for both hydrophilic PEGylated and hydrophobic surfaces. On both hydrophobic (Fig. 3, A and B) and hydrophilic (Fig. 3, C and D, and movie S1) surfaces, all droplets remained as spherical caps and dropwise condensation ensued without film formation.

To verify that contact angle hysteresis governs dropwise condensation, we performed two additional tests on surfaces having elevated advancing contact angles with varying degrees of contact angle hysteresis. The first surface consisted of a polished silicon wafer having  $\theta_a=46^\circ\pm1^\circ$  and  $\theta_r=23^\circ\pm1^\circ$ , respectively ( $\Delta\theta\approx23^\circ$ ). The droplet morphology during coalescence-mediated droplet growth showed the presence of irregular contact lines, as well as an overall quasi-dropwise condensation process (Fig. 3, E and F). A polished copper substrate (fig. S2) having a higher advancing contact angle with similar receding angle of  $\theta_a=97^\circ\pm2^\circ$  and  $\theta_r=27^\circ\pm1^\circ$ , respectively ( $\Delta\theta\approx70^\circ$ ) showed uniform filmwise condensation (Fig. 3, G and H), confirming the minimal role of advancing contact angle on dropwise condensation.

To quantify the distribution of droplet sizes during dropwise condensation, we measured the steady-state distribution of droplet sizes on both hydrophobic (Fig. 3, A and B) and hydrophilic (Fig. 3, C and D) samples. Figure 4 shows the experimentally measured droplet number density N(r) as a function of droplet radius on our hydrophilic PEGylated surface (blue circles) along with the Rose model with  $\hat{r} = r_{\rm max}/1.3 = 0.36$  mm (dashed line; condensation on the C<sub>4</sub>F<sub>8</sub> polymer) (31), valid for dropwise condensation on hydrophobic surfaces having spherical cap–shaped droplets. Our experimental data points agree well with the Rose model for multiple decades of droplet size, irrespective of the surface wettability.

## **Dropwise condensation heat transfer**

To study the impact of our findings and to quantify the effect of surface hydrophilicity on dropwise condensation heat transfer, we use an individual droplet growth model appropriate for hydrophilic dropwise condensation ( $\theta_a < 90^\circ$ ) and combine it with droplet distribution theory using the experimental distribution results for both our PEGylated and hydrophobic surfaces characterized here (section S2). As suggested in Fig. 1C and shown in the inset of Fig. 4, the utilization of a hydrophilic droplet morphology during dropwise condensation of pure steam shows a 500% heat transfer enhancement when compared to a surface having identical droplet distribution but with a hydrophobic droplet morphology. Flatter spherical cap-shaped droplets enable the minimization of conduction heat transfer resistance through the droplet, which becomes a fundamental bottleneck once droplets grow to radii above  $R \approx 10 \,\mu\text{m}$ . Study of the cumulative heat transfer shows that more than 90% of the heat removed from a surface occurs by droplets having radii  $R < 100 \mu m$ , putting high importance on minimizing advancing contact angle (32), while maintaining dropwise condensation. Note that although past researchers have suggested that lowering of the advancing contact angle was the key to dropwise condensation heat transfer increase, assumptions related to the need for intrinsic hydrophobicity for achieving stable dropwise condensation precluded the analysis of hydrophilic substrates ( $\theta_a$  < 90°) due to the assumption of dropwise-to-filmwise condensation transition (12, 28).

### **Dropwise condensation model**

We now address the fundamental question of how solid surface wettability and contact angle hysteresis govern dropwise condensation. During condensation, we expect a partial wetting condensate liquid to spread to minimize the system free energy. For small liquid volumes, i.e., when the Bond number is less than 1 (Bo  $\leq$  1), capillarity is the dominant driving force, leading to hemispherical droplet shapes (33). As the condensate grows, i.e., Bo  $\gg$  1, gravity becomes the dominant driving force in the condensate bulk (34, 35). In the gravitydominated regime (Bo  $\gg$  1), the hemispherical droplet shape approximation is no longer valid, resulting in the formation of irregular films or puddles on the condensing surface. We hypothesize that dropwise condensation is stable as long as the contact angle hysteresis-mediated droplet shedding length scale is small enough to reside in the capillarydominated regime, resulting in hemispherical droplet shapes. For surfaces having elevated contact angle hysteresis, the droplet shedding length scale is so large that capillarity ceases to govern the droplet

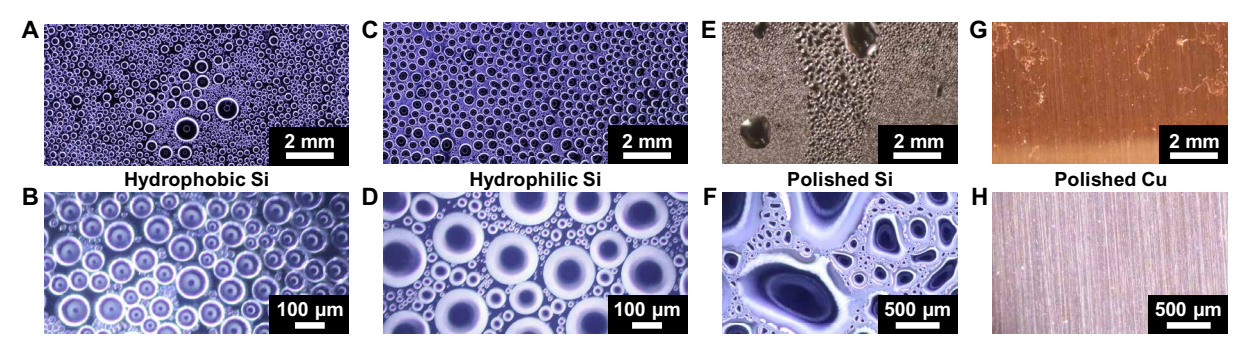
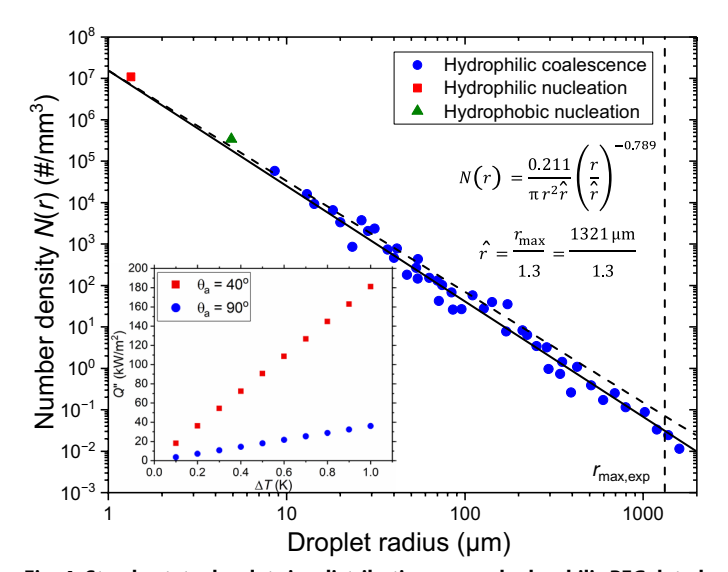


Fig. 3. Hydrophilic versus hydrophobic. Two exemplary transient droplet size distributions during condensation captured with a macro and 20× microscope lens on the (**A** and **B**) hydrophobic substrate  $(\theta_a/\theta_r = 110^\circ \pm 4^\circ/102^\circ \pm 5^\circ)$  and (**C** and **D**) PEGylated substrate  $(\theta_a/\theta_r = 38^\circ \pm 1^\circ)/35^\circ \pm 1^\circ)$ , respectively. Droplet distributions were self-similar in nature. Two exemplary transient droplet size distributions captured with a macro and 5× microscope lens on a (**E** and **F**) quasi-dropwise condensing polished silicon substrate  $(\theta_a/\theta_r = 46^\circ \pm 1^\circ/23^\circ \pm 1^\circ)$  and (**G** and **H**) filmwise condensing polished copper substrate  $(\theta_a/\theta_r = 97^\circ \pm 2^\circ/27^\circ \pm 1^\circ)$ , respectively. Experiments were conducted at a condensation heat transfer rate of  $930 \pm 100 \text{ W/m}^2$ .



**Fig. 4. Steady-state droplet size distribution on our hydrophilic PEGylated surface.** The dashed line shows the Rose distribution for hydrophobic surfaces with  $\hat{r} = r_{\text{max}}/1.3 = 0.36\,\text{mm}$  (valid for condensation on the C<sub>4</sub>F<sub>8</sub> hydrophobic polymer), and the solid line shows the fit from the inset equation. The vertical dashed line shows the experimental maximum droplet radius ( $r_{\text{max}, \text{exp}} = 1.32\,\text{mm}$ ). The droplet number density at the onset of nucleation for our PEGylated (red square symbol) and hydrophobic (green triangle symbol) surfaces are shown as well. We estimate the error associated with the automated droplet detection to be less than 10%. Experiments conducted in the presence of noncondensable gases for a condensation heat transfer rate of 930 ± 100 W/m². Inset: Model results showing overall surface condensation heat flux (Q'') as a function of vapor-to-surface temperature difference (ΔT) during dropwise condensation of pure steam on the hydrophobic (red circles) and PEGylated hydrophilic (blue squares) surfaces.

dynamics, giving way to the gravity-dominated regime (Bo  $\gg$  1) and puddle formation on the surface, resulting in filmwise condensation (Fig. 3, E and F).

To test our hypothesis, we calculated Bo for droplets immediately before departure from a vertical condensing surface to determine whether the largest droplets reside in the capillarity-dominated (Bo  $\leq$  1) or gravity-dominated (Bo  $\gg$  1) regime. We define the capillary length as  $l_y = \sqrt{\gamma/\rho g}$ , where  $\gamma$  and  $\rho$  are the condensate surface tension and density, respectively, and g is the gravitational

constant. The droplet Bond number is defined as Bo =  $R_f^2/l_V^2$  where  $R_f$ is the characteristic lateral length of the liquid droplet, taken to be its final equilibrium radius immediately before departure. The droplet radius scales as  $R_{\rm f} \sim V^{1/3}$  in the capillary-dominated regime and  $\sim V/h_*^{1/2}$ in the gravity-dominated regime, where V is the droplet volume and  $h_*$  is the puddle height (36). For the dropwise-to-filmwise transition studied here, the capillary-dominated droplet radius scaling was used as the transition is hypothesized to occur at Bo  $\approx 1$  where the shedding model remains valid for discrete droplets. The surface wettability-dependent droplet volume is defined as  $V = \pi R_f^3 (2 - 3 \cos \theta_e +$  $\cos^3\theta_e$ )/(8sin<sup>3</sup> $\theta_e$ ), where  $\theta_e = \cos^{-1}(0.5\cos\theta_a + 0.5\cos\theta_r)$  is the equilibrium contact angle immediately before shedding from the condensing surface (37). The droplet departure size  $R_f$  was calculated from a force balance between the gravitational body and contact line pinning forces and is defined as  $R_f = [6\gamma(\cos\theta_r - \cos\theta_a)\sin\theta_e)/(\pi\rho g(2-3\cos\theta_e +$  $\cos^3\theta_e$ ))]<sup>1/2</sup>. Taking the dependence of the contact angle hysteresis on the droplet volume and departure radius into account, we see a clear Bo-mediated boundary separating filmwise from dropwise condensation based on previous experimental results (Fig. 5). Our model predicts  $Bo_{crit} \approx 1.4$  as the transition boundary, with  $Bo \leq 1.4$  indicating capillary-dominated hemispherical droplet shapes at departure and Bo > 1.4 indicating gravitationally dominated puddle formation and filmwise condensation. Note that rivulet formation falls within our definition of filmwise condensation as rivulets eventually turn to films at higher subcooling. For full model development, see section S3.

#### **DISCUSSION**

The implications of our finding have substantial repercussions. Recent focus by researchers to create droplet-jumping surfaces to remove condensate at micrometer length scales has been fraught with barriers due to nucleation-mediated flooding (38), progressive flooding (39), droplet return due to gravity, and high conduction thermal resistance of droplets residing in the spherical superhydrophobic states (Fig. 1A) (28, 40). Jumping droplet condensation was only able to achieve 30% enhancement in heat transfer coefficient compared to dropwise condensation due mainly to the high apparent advancing contact angle of microscale droplets (41). Our work paves a new direction, whereby tailoring of the contact angle hysteresis, coupled with elevated nucleation density caused by high intrinsic wettability, can enhance condensation heat transfer by 500%.

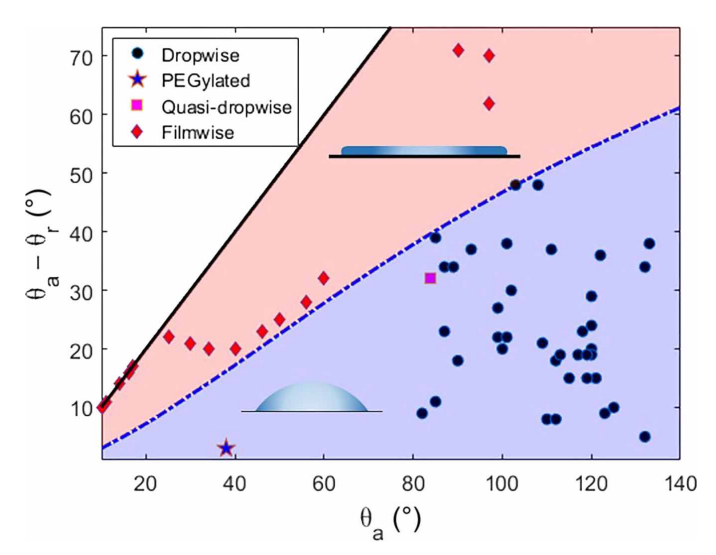


Fig. 5. Condensation regime map as a function of advancing contact angle,  $\theta_a$ , and contact angle hysteresis,  $\theta_a - \theta_r$ . The light blue and light red shaded regions represent dropwise and filmwise condensation, respectively. The dashed blue line represents Bo = 1.4. Data points in the regime map were obtained from previous works as well as this study (table S1).

In summary, we have clarified the physics behind dropwise condensation on solid surfaces, particularly highlighting the distinct role of contact angle hysteresis on dropwise-to-filmwise transitions, which are not captured by conventional advancing contact angle measurements. We demonstrated stable dropwise condensation of steam on solid hydrophilic surfaces. The experimental data revealed no statistical difference between the droplet size distribution for hydrophobic and hydrophilic substrates having low contact angle hysteresis. The discrete droplet formation we observe reinforces a picture where dropwise condensation is governed mainly by contact angle hysteresis and is fundamentally not limited by hydrophobicity or advancing contact angle. Our puddle formation model highlights the importance of the wettability-dependent departing droplet Bond number that dictates capillary- to gravity-dominated regime crossover and dropwise-to-filmwise transition at Bo≤ 1.4. The outcomes of this work not only show the important effects of surface wettability on the condensation process but also present an alternate pathway for the development of durable low-adhesion coatings on intrinsically wetting substrates such as metals, ceramics, and oxides (42).

## **MATERIALS AND METHODS**

#### **PEGylation of surfaces**

Silicon wafers ( $\langle 100 \rangle$  orientation) were cut into 2 cm by 2 cm pieces, cleaned by sonication in acetone and ethanol, rinsed with DI water, and dried with nitrogen. For PEGylation, cleaned silicon wafers were exposed to oxygen plasma (Plasma Etch) for 15 min and subsequently immersed in a solution consisting of 1  $\mu$ l of 2-[methoxy (polyethyleneoxy)6-9propyl]trimethoxysilane and 8  $\mu$ l of hydrochloric acid in 10 ml of anhydrous toluene for 18 hours at room temperature. Last, the PEGylated surfaces were rinsed thoroughly with anhydrous toluene, ethanol, and DI water and stored in DI water for further use.

## **Hydrophobic surfaces**

Smooth silicon wafers (P type,  $\langle 1\ 0\ 0 \rangle$  orientation, 0 to 100 ohm-cm, single side polished) were used as the base substrate. The wafers were first cleaned with acetone, isopropyl alcohol (IPA), and DI water and then dried with nitrogen. The wafers were descummed by oxygen plasma (March Jupiter RIE; 150 W) for 2 min to remove all remaining organic residues. After cleaning the surfaces completely, a conformal layer of octafluorocyclobutane ( $C_4F_8$ ) was coated on the surfaces by chemical vapor deposition using STS Pegasus DRIE to uniformly functionalize the surfaces to be hydrophobic. The thickness of  $C_4F_8$  was proportional to deposition time, and 3-min deposition yielded about 100 nm thickness.

### Hydrophilic silicon wafer

Smooth silicon wafers (P type, ⟨1 0 0⟩ orientation, 0 to 100 ohm·cm, single side polished) were cleaned with acetone, IPA, and DI water and then dried with nitrogen. Afterward, the wafers were treated with air plasma for 10 min before being left out uncovered in a lab environment in Urbana, IL (40°06′14″N, 88°12′44″W) to adsorb hydrocarbons and VOCs for 1 week (13–15).

#### Hydrophobic polished copper

Smooth, single side polished copper tabs (McMaster-Carr, Mirror-Like Multipurpose 110 Copper Sheets polished on one side to a reflective, mirror-like finish) were cleaned with acetone, IPA, and DI water and then dried with nitrogen. Afterward, the copper tabs were treated with air plasma for 10 min before being left out uncovered in a lab environment in Urbana, IL (40°06′14″N, 88°12′44″W) to adsorb hydrocarbons and VOCs for 1 week (13-15). Figure S2 shows AFM scans of multiple locations on the polished Cu surface, indicating a low level of nanoscale roughness. The high levels of contact angle hysteresis arose because of the nature of functionalization. We did not use a promoter coating to deposit a hydrophobic chemistry to achieve high advancing contact angles. Instead, we used hydrocarbon adsorption of VOCs to create a low surface coverage of hydrophobic molecules with large patchy areas of highsurface energy substrate exposed, resulting in substantial contact line pinning in the receding state and hence large contact angle hysteresis.

## X-ray photoelectron spectroscopy

XPS analysis was conducted on the surfaces using a PHI-5800 spectrometer (Physical Electronics). XPS was conducted using a monochromatic Al K $\alpha$  x-ray source operated at 15 kV, and photoelectrons were collected at a takeoff angle of  $\approx$ 45° relative to the sample surface. At least 30 different locations were analyzed to assess the chemical homogeneity of the PEGylated surfaces.

# **Atomic force microscopy**

The surface morphology and the surface roughness of the substrates were characterized with AFM (Bruker MultiMode 8-HR). AFM was conducted with silicon nitride probes mounted on cantilevers in the ScanAsyst mode. AFM images were acquired by scanning 5  $\mu$ m by 5  $\mu$ m areas on the PEGylated surfaces in air, under ambient laboratory conditions, at a scan rate of 1 Hz. The images were analyzed with NanoScope Analysis 1.8 software to obtain the root mean square roughness  $R_{\rm rms}$ . At least 30 different locations were analyzed to assess the roughness of the PEGylated surfaces.

#### Measurement of macroscopic contact angles

The contact angles were measured using a contact angle goniometer (ramé-hart 200-F1). The contact angles were measured by advancing or receding ~8-µl droplets on the surface. At least six measurements were performed on each surface.

#### Measurement of microscopic contact angles

Contact angle measurements of  $\approx$ 100-nl droplets on all samples were performed using a microgoniometer (MCA-3, Kyowa Interface Science). At least six measurements were performed on each surface.

#### **SUPPLEMENTARY MATERIALS**

Supplementary material for this article is available at http://advances.sciencemag.org/cgi/content/full/6/2/eaax0746/DC1

Section S1. Surface energy of PEGylated surfaces

Section S2. Dropwise condensation heat transfer

Section S3. Dropwise condensation model

Fig. S1. Time-lapse images of droplet nucleation and departure.

Fig. S2. Atomic force microscopy.

Fig. S3. Condensation regime map.

Table S1. Promoter coatings and their wetting properties.

Movie S1. Dropwise condensation on hydrophilic surface.

References (43-70)

#### REFERENCES AND NOTES

- E. Schmidt, W. Schurig, W. Sellschopp, Condensation of water vapour in film- and drop form. VDI Z. 74, 544–544 (1930).
- J. W. Rose, Dropwise condensation theory and experiment: A review. Proc. Inst. Mech. Eng. J. 216, 115–128 (2002)
- M. Alwazzan, K. Egab, B. Peng, J. Khan, C. Li, Condensation on hybrid-patterned copper tubes (I): Characterization of condensation heat transfer. *Int. J. Heat Mass Transfer* 112, 991–1004 (2017).
- M. Alwazzan, K. Egab, P. Wang, Z. Shang, X. Liang, J. khan, C. Li, Condensation heat transfer on nickel tubes: The role of atomic layer deposition of nickel oxide. *Int. J. Heat Mass Transfer* 133, 487–493 (2019).
- C. Furmidge, Studies at phase interfaces. I. The sliding of liquid drops on solid surfaces and a theory for spray retention. J. Colloid Sci. 17, 309–324 (1962).
- 6. R. Dettre, Contact angle, wettability and adhesion. Adv. Chem. Ser. 43, 136 (1964).
- R. H. Dettre, R. E. Johnson Jr., Contact angle hysteresis. IV. Contact angle measurements on heterogeneous surfaces. J. Phys. Chem. 69, 1507–1515 (1965).
- 8. P.-G. d. Gennes, F. Brochard-Wyart, D. Quéré, *Capillarity and Wetting Phenomena: Drops, Bubbles, Pearls, Waves* (Springer, 2004).
- 9. L. Bocquet, E. Lauga, A smooth future? Nat. Mater. 10, 334–337 (2011).
- D. Daniel, J. V. I. Timonen, R. Li, S. J. Velling, M. J. Kreder, A. Tetreault, J. Aizenberg, Origins of extreme liquid repellency on structured, flat, and lubricated hydrophobic surfaces. *Phys. Rev. Lett.* 120, 244503 (2018).
- D. Kashchiev, Nucleation: Basic Theory with Applications (Butterworth-Heinemann, ed. 1, 2000).
- R. Xiao, N. Miljkovic, R. Enright, E. N. Wang, Immersion condensation on oil-infused heterogeneous surfaces for enhanced heat transfer. Sci. Rep. 3, 1988 (2013).
- D. J. Preston, N. Miljkovic, J. Sack, R. Enright, J. Queeney, E. N. Wang, Effect of hydrocarbon adsorption on the wettability of rare earth oxide ceramics. *Appl. Phys. Lett.* **105**, 011601 (2014).
- H. Cha, A. Wu, M. K. Kim, K. Saigusa, A. Liu, N. Miljkovic, Nanoscale-agglomerate-mediated heterogeneous nucleation. *Nano Lett.* 17, 7544–7551 (2017).
- R. Lundy, C. Byrne, J. Bogan, K. Nolan, M. N. Collins, E. Dalton, R. Enright, Exploring the role of adsorption and surface state on the hydrophobicity of rare earth oxides. ACS Appl. Mater. Interfaces 9. 13751–13760 (2017).
- 16. J. W. Rose, Condensation heat transfer fundamentals. Chem. Eng. Res. Des. 76, 143–152 (1998).
- 17. R. E. Johnson Jr., R. H. Dettre, Contact angle hysteresis. III. Study of an idealized heterogeneous surface. *J. Phys. Chem.* **68**, 1744–1750 (1964).
- S. Sharma, R. W. Johnson, T. A. Desai, XPS and AFM analysis of antifouling PEG interfaces for microfabricated silicon biosensors. *Biosens. Bioelectron.* 20, 227–239 (2004).
- T.-S. Wong, S. H. Kang, S. K. Y. Tang, E. J. Smythe, B. D. Hatton, A. Grinthal, J. Aizenberg, Bioinspired self-repairing slippery surfaces with pressure-stable omniphobicity. *Nature* 477, 443–447 (2011).
- K. Rykaczewski, A. T. Paxson, M. Staymates, M. L. Walker, X. Sun, S. Anand, S. Srinivasan, G. H. McKinley, J. Chinn, J. H. J. Scott, K. K. Varanasi, Dropwise condensation of low surface tension fluids on omniphobic surfaces. *Sci. Rep.* 4, 4158 (2014).

- B. R. Solomon, S. B. Subramanyam, T. A. Farnham, K. S. Khalil, S. Anand, K. K. Varanasi, in Non-Wettable Surfaces: Theory, Preparation and Applications (The Royal Society of Chemistry, 2017), pp. 285–318.
- S. Anand, A. T. Paxson, R. Dhiman, J. D. Smith, K. K. Varanasi, Enhanced condensation on lubricant-impregnated nanotextured surfaces. ACS Nano 6, 10122–10129 (2012).
- F. Schellenberger, J. Xie, N. Encinas, A. Hardy, M. Klapper, P. Papadopoulos, H. J. Butt, D. Vollmer, Direct observation of drops on slippery lubricant-infused surfaces. Soft Matter 11, 7617–7626 (2015).
- C. Semprebon, G. McHale, H. Kusumaatmaja, Apparent contact angle and contact angle hysteresis on liquid infused surfaces. Soft Matter 13, 101–110 (2017).
- S. Sett, X. Yan, G. Barac, L. W. Bolton, N. Miljkovic, Lubricant-infused surfaces for lowsurface-tension fluids: Promise versus reality. ACS Appl. Mater. Interfaces 9, 36400–36408 (2017)
- P. B. Weisensee, Y. Wang, H. Qian, D. Schultz, W. P. King, N. Miljkovic, Condensate droplet size distribution on lubricant-infused surfaces. *Int. J. Heat Mass Transfer* 109, 187–199 (2017).
- M. K. Kim, H. Cha, P. Birbarah, S. Chavan, C. Zhong, Y. Xu, N. Miljkovic, Enhanced jumping-droplet departure. *Langmuir* 31, 13452–13466 (2015).
- S. Chavan, H. Cha, D. Orejon, K. Nawaz, N. Singla, Y. F. Yeung, D. Park, D. H. Kang, Y. Chang, Y. Takata, N. Miljkovic, Heat transfer through a condensate droplet on hydrophobic and nanostructured superhydrophobic surfaces. *Langmuir* 32, 7774–7787 (2016).
- E. Ölçeroğlu, M. McCarthy, Spatial control of condensate droplets on superhydrophobic surfaces. J. Heat Transfer 137, 080905 (2015).
- K. K. Varanasi, M. Hsu, N. Bhate, W. S. Yang, T. Deng, Spatial control in the heterogeneous nucleation of water. *Appl. Phys. Lett.* 95, 094101 (2009).
- J. W. Rose, L. R. Glicksman, Dropwise condensation—The distribution of drop sizes. Int. J. Heat Mass. Transf. 16, 411–425 (1973).
- 32. A. Umur, P. Griffith, Mechanism of dropwise condensation. *J. Heat Transfer* **87**, 275–282 (1965).
- 33. L. H. Tanner, The spreading of silicone oil drops on horizontal surfaces. *J. Phys. D Appl. Phys.* **12**, 1473–1484 (1979).
- J. Lopez, C. A. Miller, E. Ruckenstein, Spreading kinetics of liquid-drops on solids. J. Colloid Interface Sci. 56, 460–468 (1976).
- L. M. Hocking, The spreading of a thin drop by gravity and capillarity. Q. J. Mech. Appl. Math.
   36. 55–69 (1983).
- A. Alizadeh Pahlavan, L. Cueto-Felgueroso, G. H. McKinley, R. Juanes, Thin films in partial wetting: Internal selection of contact-line dynamics. *Phys. Rev. Lett.* 115, 034502
- R. Enright, N. Miljkovic, N. Dou, Y. Nam, E. N. Wang, Condensation on superhydrophobic copper oxide nanostructures. J. Heat Transfer. 135, 091304 (2013).
- E. Ölçeroğlu, M. McCarthy, Self-organization of microscale condensate for delayed flooding of nanostructured superhydrophobic surfaces. ACS Appl. Mater. Interfaces 8, 5779–5736 (2016)
- N. Miljkovic, D. J. Preston, R. Enright, E. N. Wang, Electric-field-enhanced condensation on superhydrophobic nanostructured surfaces. ACS Nano 7, 11043–11054 (2013).
- R. Enright, N. Miljkovic, J. L. Alvarado, K. J. Kim, J. W. Rose, Dropwise condensation on micro- and nanostructured surfaces. *Nanosc. Mircosc. Therm. Eng.* 8, 223–250 (2014).
- N. Miljkovic, R. Enright, Y. Nam, K. Lopez, N. Dou, J. Sack, E. N. Wang, Jumping-dropletenhanced condensation on scalable superhydrophobic nanostructured surfaces. *Nano Lett.* 13, 179–187 (2012).
- R. Tadmor, R. Das, S. Gulec, J. Liu, H. E. N'guessan, M. Shah, P. S. Wasnik, S. B. Yadav, Solid-liquid work of adhesion. *Langmuir* 33, 3594–3600 (2017).
- D. K. Owens, R. C. Wendt, Estimation of the surface free energy of polymers. J. Appl. Polym. Sci. 13. 1741–1747 (1969).
- B. Jańczuk, W. Wójcik, A. Zdziennicka, Determination of the components of the surface tension of some liquids from interfacial liquid-liquid tension measurements. J. Colloid Interface Sci. 157, 384–393 (1993).
- S. S. Sadhal, W. W. Martin, Heat transfer through drop condensate using differential inequalities. Int. J. Heat Mass Transfer 20, 1401–1407 (1977).
- 46. R. W. Schrage, thesis, Columbia University, New York (1953).
- J. W. Rose, On interphase matter transfer, the condensation coefficient and dropwise condensation. Proc. R. Soc. London, Ser. A 411, 305–311 (1987).
- S. Kim, K. J. Kim, Dropwise condensation modeling suitable for superhydrophobic surfaces. J. Heat Transfer 133, 081502 (2011).
- E. J. Le Fevre, J. W. Rose, in Proceedings of the Third International Heat Transfer Conference (ASME, 1966), vol. 2, pp. 362–375.
- N. Miljkovic, R. Enright, E. N. Wang, Modeling and optimization of superhydrophobic condensation. J. Heat Transfer 135, 111004 (2013).
- H. E. Huppert, The propagation of two-dimensional and axisymmetric viscous gravity currents over a rigid horizontal surface. J. Fluid Mech. 121, 43–58 (1982).

# SCIENCE ADVANCES | RESEARCH ARTICLE

- X. Yan, Z. Huang, S. Sett, J. Oh, H. Cha, L. Li, L. Feng, Y. Wu, C. Zhao, D. Orejon, F. Chen, N. Miljkovic, Atmosphere-mediated superhydrophobicity of rationally designed micro/ nanostructured surfaces. ACS Nano 13, 4160–4173 (2019).
- X. H. Ma, J. Chen, D. Xu, J. Lin, C. Ren, Z. Long, Influence of processing conditions of polymer film on dropwise condensation heat transfer. *Int. J. Heat Mass Transfer* 45, 3405–3411 (2002).
- K. M. Holden, A. S. Wanniarachchi, P. J. Marto, D. H. Boone, J. W. Rose, The use of organic coatings to promote dropwise condensation of steam. J. Heat Transfer 109, 768–774 (1987).
- A. T. Paxson, J. L. Yague, K. K. Gleason, K. K. Varanasi, Stable dropwise condensation for enhancing heat transfer via the initiated chemical vapor deposition (icvd) of grafted polymer films. *Adv. Mater.* 26, 418–423 (2014).
- H. Cha, C. Xu, J. Sotelo, J. M. Chun, Y. Yokoyama, R. Enright, N. Miljkovic, Coalescenceinduced nanodroplet jumping. *Phys. Rev. Fluids* 1, 064102 (2016).
- D. J. Preston, D. L. Mafra, N. Miljkovic, J. Kong, E. N. Wang, Scalable graphene coatings for enhanced condensation heat transfer. *Nano Lett.* 15, 2902–2909 (2015).
- A. W. Neumann, A. H. Abdelmessih, A. Hameed, The role of contact angles and contact angle hysteresis in dropwise condensation heat transfer. *Int. J. Heat Mass Transfer* 21, 947–953 (1978)
- G. Azimi, R. Dhiman, H. K. Kwon, A. T. Paxson, K. K. Varanasi, Hydrophobicity of rare-earth oxide ceramics. *Nat. Mater.* 12, 315–320 (2013).
- M. P. Bonnar, B. M. Burnside, A. Little, R. L. Reuben, J. I. B. Wilson, Plasma polymer films for dropwise condensation of steam. *Chem. Vap. Deposition* 3, 201–207 (1997).
- Y.-L. Lee, C.-H. Chen, Y.-M. Yang, Surface morphology and wetting behavior of poly (α-methylstyrene) thin films prepared by vacuum deposition. *Langmuir* 14, 6980–6986 (1998).
- N. Miljkovic, D. J. Preston, R. Enright, E. N. Wang, Electrostatic charging of jumping droplets. *Nat. Commun.* 4, 2517 (2013).
- A. B. Ponter, M. Yektafard, The influence of environment on the drop size—Contact-angle relationship. Colloid Polym. Sci. 263, 673–681 (1985).
- R. F. Wen, Z. Lan, B. Peng, W. Xu, X. Ma, Y. Cheng, Droplet departure characteristics and dropwise condensation heat transfer at low steam pressure. *J. Heat Transfer* 138, 071501 (2016).
- A. P. Boyes, A. B. Ponter, Wettability of copper and polytetrafluoroethylene surfaces with water— The influence of environmental conditions. *Chem. Ing. Tech.* 45, 1250–1256 (1973).

- G. D. Bansal, S. Khandekar, K. Muralidhar, Measurement of heat transfer during drop-wise condensation of water on polyethylene. *Nanosc. Microsc. Therm. Eng.* 13, 184–201 (2009).
- E. Hoque, J. A. DeRose, R. Houriet, P. Hoffmann, H. J. Mathieu, Stable perfluorosilane self-assembled monolayers on copper oxide surfaces: Evidence of siloxy-copper bond formation. Chem. Mater. 19, 798–804 (2007).
- M. J. Pellerite, E. J. Wood, V. W. Jones, Dynamic contact angle studies of self-assembled thin films from fluorinated Alkyltrichlorosilanes 1. J. Phys. Chem. B 106, 4746–4754 (2002).
- R. A. Erb, Wettability of metals under continuous condensing conditions. J. Phys. Chem. 69, 1306–1309 (1965).
- S. A. Stylianou, J. W. Rose, Drop-to-filmwise condensation transition: Heat transfer measurements for ethanediol. *Int. J. Heat Mass Transfer* 26, 747–760 (1983).

Acknowledgments: We thank D. Orejon of Kyushu University for reading and commenting on the manuscript. Funding: We acknowledge funding support from the Office of Naval Research (grant no. N00014-16-1-2625). We also acknowledge funding support from the International Institute for Carbon Neutral Energy Research (WPI-I2CNER), sponsored by the Japanese Ministry of Education, Culture, Sports, Science and Technology. A.K.K. acknowledges financial support under award 1751628 from the NSF and under awards R01HL135505 and R21HL139208 from the NIH. Author contributions: H.C., A.W., S.S., and S.A.B. performed the experiments. H.V. and W.W. designed and fabricated the hydrophilic surface. S.C. developed the dropwise condensation heat transfer model. M.-K.K. fabricated the hydrophobic surfaces. A.K.K. and N.M. supervised the whole work. Competing interests: The authors declare that they have no competing interests. Data and materials availability: All data needed to evaluate the conclusions in the paper are present in the paper and/or the Supplementary Materials. Additional data related to this paper may be requested from the authors.

Submitted 20 February 2019 Accepted 11 November 2019 Published 10 January 2020 10.1126/sciadv.aax0746

Citation: H. Cha, H. Vahabi, A. Wu, S. Chavan, M.-K. Kim, S. Sett, S. A. Bosch, W. Wang, A. K. Kota, N. Miljkovic, Dropwise condensation on solid hydrophilic surfaces. *Sci. Adv.* **6**, eaax0746 (2020).



# Dropwise condensation on solid hydrophilic surfaces

Hyeongyun Cha, Hamed Vahabi, Alex Wu, Shreyas Chavan, Moon-Kyung Kim, Soumyadip Sett, Stephen A. Bosch, Wei Wang, Arun K. Kota and Nenad Miljkovic

Sci Adv **6** (2), eaax0746. DOI: 10.1126/sciadv.aax0746

ARTICLE TOOLS http://advances.sciencemag.org/content/6/2/eaax0746

SUPPLEMENTARY MATERIALS http://advances.sciencemag.org/content/suppl/2020/01/06/6.2.eaax0746.DC1

This article cites 65 articles, 0 of which you can access for free http://advances.sciencemag.org/content/6/2/eaax0746#BIBL REFERENCES

PERMISSIONS http://www.sciencemag.org/help/reprints-and-permissions

Use of this article is subject to the Terms of Service